BIOCHEMISTRY
including biophysical chemistry & molecular biology
Article

Biochemistry **2011,** *50,* 591–598 591
DOI: 10.1021/bi101696h

How Coenzyme B_{12}-Dependent Ethanolamine Ammonia-Lyase Deals with Both Enantiomers of 2-Amino-1-propanol as Substrates: Structure-Based Rationalization[†,‡,▽]

Naoki Shibata,*[,§,∥] Yoshiki Higuchi,[§,∥] and Tetsuo Toraya*[,⊥]

[§]*Department of Life Science, Graduate School of Life Science, University of Hyogo, 3-2-1 Koto, Kamigori-cho, Ako-gun, Hyogo 678-1297, Japan,* [∥]*RIKEN Harima Institute, SPring-8 Center, 1-1-1 Koto, Sayo-cho, Sayo-gun, Hyogo 679-5148, Japan, and* [⊥]*Department of Bioscience and Biotechnology, Graduate School of Natural Science and Technology, Okayama University, Tsushima-naka, Kita-ku, Okayama 700-8530, Japan*

Received October 21, 2010; Revised Manuscript Received December 10, 2010

ABSTRACT: Coenzyme B_{12}-dependent ethanolamine ammonia-lyase acts on both enantiomers of the substrate 2-amino-1-propanol [Diziol, P., et al. (1980) *Eur. J. Biochem. 106*, 211−224]. To rationalize this apparent lack of stereospecificity and the enantiomer-specific stereochemical courses of the deamination, we analyzed the X-ray structures of enantiomer-bound forms of the enzyme−cyanocobalamin complex. The lower affinity for the (*R*)-enantiomer may be due to the conformational change of the Valα326 side chain of the enzyme. In a manner consistent with the reported experimental results, we can predict that the *pro-S* hydrogen atom on C1 is abstracted by the adenosyl radical from both enantiomeric substrates, because it is the nearest one in both enantiomer-bound forms. We also predicted that the NH_2 group migrates from C2 to C1 by a suprafacial shift, with inversion of configuration at C1 for both enantiomeric substrates, although the absolute configuration of the 1-amino-1-propanol intermediate is not yet known. Reported labeling experiments demonstrate that (*R*)-2-amino-1-propanol is deaminated by the enzyme with inversion of configuration at C2, whereas the (*S*)-enantiomer is deaminated with retention. By taking these results into consideration, we can predict the rotameric radical intermediate from the (*S*)-enantiomer undergoes flipping to the rotamer from the (*R*)-enantiomer before the hydrogen back-abstraction. This suggests the preference of the enzyme active site for the rotamer from the (*R*)-enantiomer in equilibration. This preference might be explained in terms of the steric repulsion of the (*S*)-enantiomer-derived product radical at C3 with the Pheα329 and Leuα402 residues.

Enzymes are generally stereospecific for their substrates, but a few enzymes are exceptional and lack stereospecificity. Adenosylcobalamin (AdoCbl,[1] coenzyme B_{12})-dependent diol dehydratase (EC 4.2.1.28) and ethanolamine ammonia-lyase (ethanolamine deaminase) (EAL, EC 4.3.1.7) are two of these enzymes. They act on both enantiomers (*1*−*8*). EAL catalyzes the AdoCbl-dependent conversion of ethanolamine to acetaldehyde and ammonia (*9*) (eq 1):

$$^{+}H_3NCH_2CH_2OH \rightarrow CH_3CHO + NH_4^{+} \quad (1)$$

Diol dehydratase catalyzes the conversion of 1,2-diols and glycerol to the corresponding aldehydes (*10*, *11*). EAL and diol dehydratase catalyze the same type of intramolecular group-transfer reactions (Figure 1A) and are thought to do so by a common minimal mechanism (Figure 1B) (X, NH_2 for EAL and OH for diol dehydratase on C2; H, hydrogen atom on C1) (*12*−*16*). That is, the enzyme−coenzyme interaction leads to the activation of the Co−C bond of the coenzyme (*17*−*20*). Substrate binding induces the additional labilization of the Co−C bond (*21*, *22*), resulting in its homolysis to form the adenosyl radical and cob(II)alamin. The adenosyl radical abstracts a hydrogen atom from the substrate, producing a substrate-derived radical and 5′-deoxyadenosine. The substrate radical rearranges to the product radical, which then abstracts a hydrogen atom back from 5′-deoxyadenosine. This leads to the formation of the product and the regeneration of the coenzyme.

Diol dehydratase acts on both (*R*)- and (*S*)-1,2-propanediols (*1*−*6*). Each enantiomer follows a different stereochemical course of reaction (*1*−*3*). We have previously rationalized the apparent lack of stereospecificity of diol dehydratase on the basis of its X-ray structure (*23*).

EAL also catalyzes the conversion of both (*R*)- and (*S*)-2-amino-1-propanol to propionaldehyde, although they are much poorer substrates than ethanolamine (*7*, *8*, *24*). Babior and coworkers reported that, when each enantiomer is run independently, the (*S*)-enantiomer shows a lower K_m and a higher V_{max} than the (*R*)-enantiomer (*7*, *8*). These results suggested that the (*R*)- and (*S*)-enantiomers are bound to the enzyme in two different modes with different catalytic efficiencies and binding affinities; that is, EAL seems to recognize the enantiomers as "different" substrates.

[†]This work was supported in part by the Global COE Program (to N.S. and Y.H.), Grants-in-Aid for Scientific Research [18GS0207 to Y.H. and (B)13480195 and (B)17370038 and Priority Area 513 to T.T.] from the Japan Society for Promotion of Science and the Ministry of Education, Culture, Sports, Science and Technology, Japan, the Core Research for Evolutional Science and Technology (CREST) Program of the Japan Science and Technology Agency (to Y.H.), and a Grant-in-Aid for Natural Sciences Research (to T.T.) from the Asahi Glass Foundation (Tokyo, Japan). This work was performed using synchrotron beamline BL44XU at SPring-8 under the Cooperative Research Program of the Institute for Protein Research, Osaka University (Osaka, Japan).

[‡]The coordinates and structure factors have been deposited in the Protein Data Bank as entries 3ANY [CN-Cbl−(*R*)-2-amino-1-propanol complex] and 3AO0 [CN-Cbl−(*S*)-2-amino-1-propanol complex].

[▽]Dedicated to the Emeritus Professor János Rétey for pioneering work.

*To whom correspondence should be addressed. T.T.: telephone, 81-86-251-8194; fax, 81-86-251-8196; e-mail, toraya@cc.okayama-u.ac.jp. N.S.: telephone, 81-791-58-0178; fax, 81-791-58-0563; e-mail, shibach@sci.u-hyogo.ac.jp.

[1]Abbreviations: AdoCbl, adenosylcobalamin or coenzyme B_{12}; CN-Cbl, cyanocobalamin; EAL, ethanolamine ammonia-lyase.

Published on Web 12/10/2010

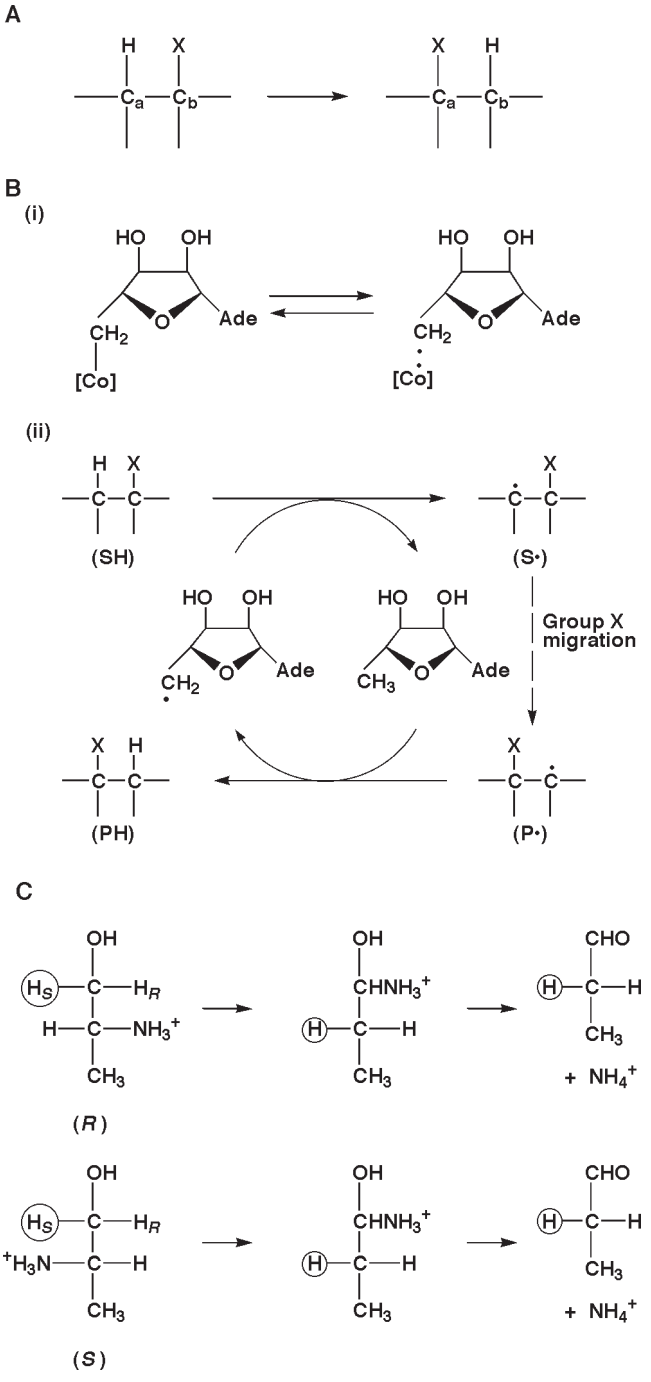

FIGURE 1: General representation (A) and minimal mechanism (B) of AdoCbl-dependent rearrangements and stereochemical features of the 2-amino-1-propanol deamination catalyzed by EAL (C). H_R and H_S represent the *pro-R* and *pro-S* hydrogens, respectively.

Rétey, Babior, and co-workers established the stereochemical courses of the EAL reaction with labeling experiments (*25*). The essential points can be summarized in Figure 1C. (i) The *pro-S* hydrogen atom on C1 is stereospecifically abstracted from both (*R*)- and (*S*)-enantiomers. (ii) EAL deaminates (*R*)-2-amino-1-propanol with inversion of configuration at C2, whereas the (*S*)-enantiomer reacts with retention. Such stereochemical courses of the EAL reaction are quite different from those of the diol dehydratase reaction (*1*−*3*, *23*). When chirally labeled (*R*)- and (*S*)-[2-^{2}H,^{3}H]ethanolamines were used as substrates, the chirality of C2 was lost (*26*). This finding indicates the involvement of a rotating methylene radical intermediate whose rapid internal rotation occurs before the hydrogen back-abstraction, i.e., torsion symmetry.

Recently, we determined the X-ray structures of EAL in complexes with cyanocobalamin (CN-Cbl) or adeninylpentylcobalamin (AdePeCbl) with and without the substrate ethanolamine (*22*). The structure of the EAL−CN-Cbl complex with racemic 2-amino-1-propanol was also determined, but it was not clear which enantiomer is predominantly bound to the active site of EAL. To rationalize the enantiomer-specific stereochemical courses of the 2-amino-1-propanol deamination, we analyzed the X-ray structures of enantiomer-bound forms of the EAL−CN-Cbl complexes. In addition, the conformations of the enzyme-bound 1-amino-1-propanol intermediates from enantiomeric substrates were modeled. On the basis of these X-ray structures and models, we propose here the stereochemical courses of the EAL reaction with the (*R*)- and (*S*)-enantiomers, which account for why EAL apparently lacks specificity for the enantiomers of its substrates.

EXPERIMENTAL PROCEDURES

Materials. CN-Cbl was purchased from Sigma-Aldrich (St. Louis, MO). The polyethylene glycol 4000 solution was from Hampton Research (Aliso Viejo, CA). All other chemicals were from Wako Pure Chemical Industries, Ltd. (Osaka, Japan), unless otherwise stated.

Enzyme Purification. *Escherichia coli* JM109 cells carrying pUSI2ENd(EAL(Δβ4−43)) plasmid were used for homologous overexpression of *E. coli* EAL(βΔ4−43) which consists of the α subunit and the N-terminal His6-tagged β subunit lacking residues Lysβ4−Cysβ43 (*27*). Purification of EAL(βΔ4−43) was achieved via affinity chromatography on Ni-NTA agarose (Qiagen) and size-exclusion chromatography, as described previously (*27*). The final protein solution contained 20 mg/mL enzyme, 10 mM Tris-HCl buffer (pH 8.0) containing 200 mM KCl, 1 mM dithiothreitol (DTT), and 20 μM CN-Cbl.

Crystallization. Crystals of the EAL(Δβ4−43)−CN-Cbl complex bound to (*R*)- or (*S*)-2-amino-1-propanol were prepared by the following procedure. Briefly, crystals of the substrate-free form of the EAL(Δβ4−43)−CN-Cbl complex were obtained by the sitting drop vapor diffusion method using a well solution containing 6.0−7.0% (w/v) polyethylene glycol 4000, 24−26% (v/v) glycerol, 1.0% (v/v) 2-methyl-2,4-pentanediol (MPD), and 0.1 M imidazole-HCl (pH 6.3), as described previously (*27*). Thus obtained substrate-free crystals were harvested and soaked for 30 min in the mother liquor supplemented with 10 mM (*R*)- or (*S*)-2-amino-1-propanol (pH 8.0) as well as each component of the substrate-free final buffer.

Data Collection. X-ray diffraction data collection was performed at beamline BL44XU (SPring-8, Hyogo, Japan). Prior to diffraction experiments, the crystals were flash-cooled with a nitrogen gas stream at 100 K. Diffraction data sets were indexed, integrated, and scaled using HKL2000 (*28*). Diffraction data from the crystals of the CN-Cbl−(*R*)-2-amino-1-propanol and CN-Cbl−(*S*)-2-amino-1-propanol complexes were collected up to 2.10 and 2.25 Å, respectively. Detailed statistics of the X-ray crystallography experiments are listed in Table S1 of the Supporting Information.

Structural Refinement. The model of substrate-free EAL with water molecules removed was used for the first refinement step. Clear electron densities corresponding to (*R*)- and (*S*)-2-amino-1-propanols were observed in the $F_o - F_c$ electron density maps of both complexes. The model was improved by iterative

rounds of refinement using REFMAC5 (*29*) and model rebuilding using COOT (*30*) until the R_{free} value decreased to less than 30%. At this stage, TLS refinement using REFMAC5 was applied to the model, and several further refinement cycles yielded the final model. Statistics for refinement are listed in Table S1 of the Supporting Information. The model figures were generated using CHIMERA (*31*). Ramachandran plot statistics and χ angles for residues were calculated with Molprobity (*32*).

Modeling of 1-Amino-1-propanol. Models for the 1-amino-1-propanol-bound forms of EAL were generated according to the previously reported method (*23*). 1-Amino-1-propanol models built with COOT were subjected to hydrogen generation and energy minimization using CNS (*33*). The hydrogen-generated models were then fit into the 2-amino-1-propanol model so that their amino and hydroxyl groups are as close as possible to their respective groups of 2-amino-1-propanol.

RESULTS AND DISCUSSION

Modes of Binding of (R)- and (S)-2-Amino-1-propanol to EAL. Both (*R*)- and (*S*)-2-amino-1-propanol are bound at the substrate-binding site in the $(\beta/\alpha)_8$ or TIM barrel of the α subunit, as reported previously (Figure S1 of the Supporting Information and Figure 2) (*22*). As expected, the shapes of the electron density of each enantiomer were significantly different from each other. The electron densities of their methyl groups (C3 atom) projected out toward the side chain of Valα326 in the (*R*)-enantiomer-bound form, whereas toward that of Pheα329 in the (*S*)-enantiomer-bound form (Figure 2). The other part of both enantiomers is oriented in approximately the same direction, and differences in the position of each corresponding atom between both enantiomers are small in the amino (N2 atom, 0.09 Å) and hydroxyl (O1 atom, 0.32 Å) groups and the C1 atom (0.39 Å) but relatively large in the C2 (0.71 Å) and C3 (1.11 Å) atoms. The amino acid residues that form hydrogen bonds with the substrate molecule are essentially the same in both forms. The amino and hydroxyl groups form three hydrogen bonds with Glnα162, Gluα287, and Aspα362 and with Argα160, Asnα193, and Gluα287, respectively.

If the following ranges are used to classify the conformers by dihedral angles (*syn*, 0 ± 30°; *anti*, 180 ± 30°; *positive gauche*, 60 ± 30°; *negative gauche*, −60 ± 30°) (*34*), one significant structural difference between (*R*)- and (*S*)-enantiomer-bound forms is that the side chain of Valα326 has a *negative gauche* (χ_1 = 298.9°) conformation in the (*R*)-enantiomer-bound form but a nearly *anti* (χ_1 = 207.7°) conformation in the (*S*)-enantiomer-bound form. The closest atom of the substrate molecule from Valα326 is C3 in both (*R*)- and (*S*)-enantiomer-bound forms, and their C3−Valα326 distances are very similar (3.58 and 3.62 Å, respectively). On the other hand, superimposed models of these forms showed that the C3 atom of the (*R*)-enantiomer has a shorter contact with Valα326 than in the (*S*)-enantiomer-bound form (3.32 Å), suggesting that the *anti* conformer of Valα326 causes stronger steric repulsion against the (*R*)-enantiomer than the *negative gauche* conformer. Moreover, Valα326 in the substrate-free form (*22*) shows an *anti* (χ_1 = 197.4°) conformation, indicating that this residue has the *anti* conformation before substrate binding. In the case of the ethanolamine-bound form (*22*),

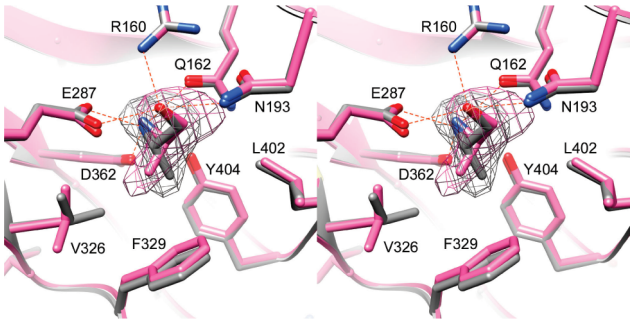

FIGURE 2: Sigma-A-weighted $F_o - F_c$ electron density maps at the substrate binding site of the EAL(Δβ4−43)−CN-Cbl complex bound to (*R*)-2-amino-1-propanol (pink) or (*S*)-2-amino-1-propanol (gray). The maps after the first refinement without substrate are contoured at the 3σ level. Schematics of the final models are shown.

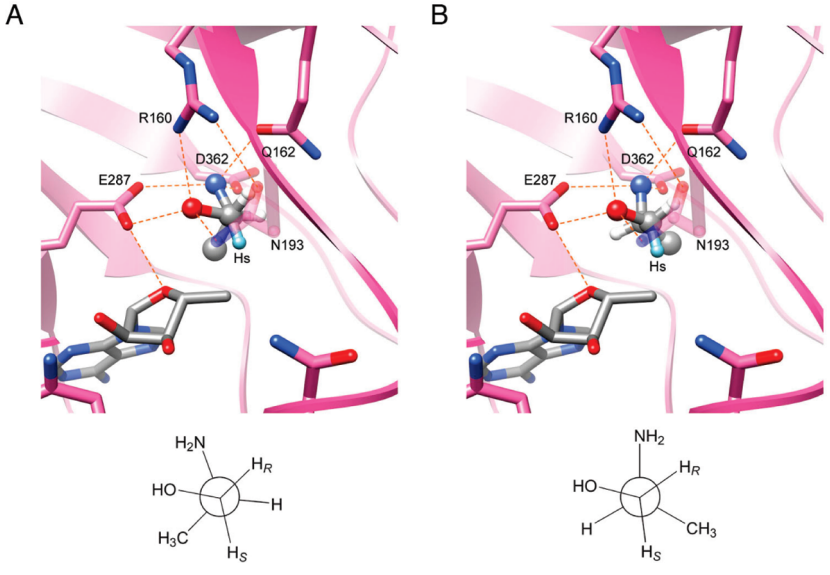

FIGURE 3: Nearest hydrogen atom to be abstracted from (*R*)-2-amino-1-propanol (A) and (*S*)-2-amino-1-propanol (B) by the adenosyl radical. In the top panels, 2-amino-1-propanol models are shown in ball-and-stick representation with atom color except for H_S (sky blue). The hydrogen atoms of 2-amino-1-propanol models were generated using CNS (*33*). The adenosyl radical model represented by an atom-colored stick model is derived from the structure of EAL complexed with adeninylpentylcobalamin and ethanolamine (*22*). CN-Cbl and the residues at the substrate-binding site are drawn as stick models and colored pink for carbon atoms and by atom for the others. The bottom panels display Newman projections of the hydrogen-generated 2-amino-1-propanol models. H_R and H_S represent the *pro-R* and *pro-S* hydrogens, respectively.

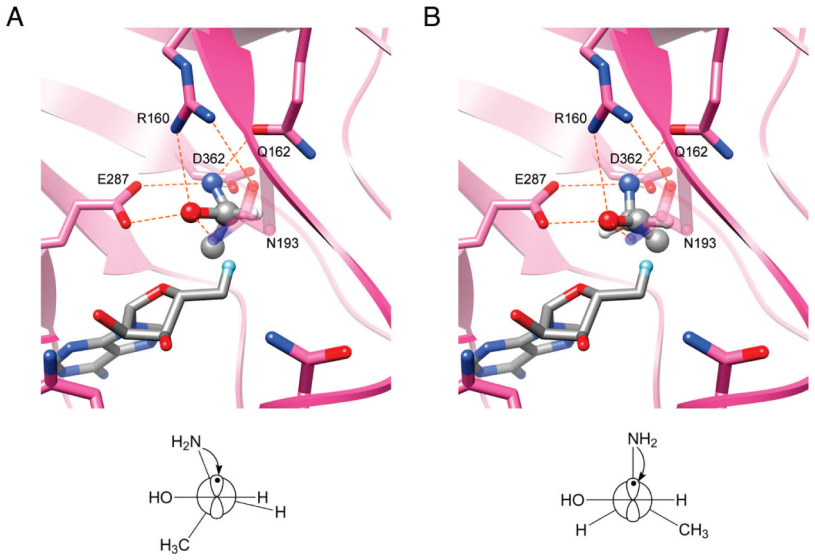

FIGURE 4: Modeling of the substrate-derived radicals and suprafacial 1,2-shifts of the amino group on C2 for (A) (*R*)-2-amino-1-propanol-1-yl radical and (B) (*S*)-2-amino-1-propanol-1-yl radical.

Valα326 has a nearly *anti* (χ_1 = 208.0°) conformation and less steric repulsion from ethanolamine (3.80 Å from the C2 atom of ethanolamine) than from (*R*)-2-amino-1-propanol. These lines of evidence suggest that the (*R*)-enantiomer needs to switch the conformation of Valα326 from *anti* to *negative gauche* to weaken the steric repulsion upon binding to the enzyme, whereas the (*S*)-enantiomer and ethanolamine do not. Both ethanolamine and (*S*)-2-amino-1-propanol have lower K_m values than (*R*)-2-amino-1-propanol (*7*, *8*). We concluded that the energy cost for changing the conformation of Valα326 from *anti* to *negative gauche* contributes to the higher K_m value for (*R*)-2-amino-1-propanol than for the other substrates.

In a previous work (*22*), we reported that the electron density map was not sufficiently clear to distinguish which enantiomer of 2-amino-1-propanol was predominantly bound to EAL in the presence of the racemic compound. However, the shape of the electron density map for the substrate molecule in the presence of racemic 2-amino-1-propanol looks more similar to that of the (*S*)-enantiomer than that of the (*R*)-enantiomer. This result suggests that the (*S*)-enantiomer was predominantly bound even in the presence of the (*R*)-enantiomer at an equal concentration, which is consistent with the previous report that the (*S*)-enantiomer has a lower K_m value than the (*R*)-enantiomer (*7*, *8*). This is supported by the fact that the conformation of the side chain of Valα326 is in the *anti* (χ_1 = 205.1°) conformation in the racemic 2-amino-1-propanol structure.

Stereospecificity of Abstraction of Hydrogen from Substrates. Diziol et al. (*25*) reported that a large KIE ($k_H/k_D \sim 6$) was observed with (*S*)-2-amino-[1,1-$^2H_2$]1-propanol and (1*S*,2*S*)-2-amino-[1-$^2H_1$]1-propanol, but not with (1*R*,2*S*)-2-amino-[1-$^2H_1$]1-propanol. (*R*)-2-Amino-[1,1-$^2H_2$]1-propanol reacts ~1.7 times more slowly than unlabeled (*R*)-2-amino-1-propanol or (1*R*,2*R*)-2-amino-[1-$^2H_1$]1-propanol. These results indicate that (i) enantiomeric 2-amino-[1,1-$^2H_2$]1-propanols react at the same rate and (ii) the *pro-S* hydrogen atom on C1 is stereospecifically abstracted from both (*R*)- and (*S*)-enantiomers. The enzyme-bound AdoCbl serves as an intermediate hydrogen carrier, first accepting a hydrogen atom from C1 of substrates to C5′ of the coenzyme and then, in a subsequent step, giving a hydrogen back to C2 of the product (*12*−*16*). Panels A and B of Figure 3 show the structures of the active sites of the (*R*)- and (*S*)-enantiomer-bound forms of the EAL−cobalamin complex, respectively. The ribosyl rotation model may explain not only the radical−substrate distance problem but also the specificity of the hydrogen abstraction as in diol dehydratase (*23*, *35*). The position of the adenosyl radical in the hydrogen-abstracting ("distal") conformation is also shown together. This was previously obtained by the modeling study (*22*); that is, the adenine moiety of the coenzyme adenosyl group was superimposed on the adenine-binding pocket of EAL, and the ribose moiety was rotated around the glycosidic linkage so that the distance between C5′ of 5′-deoxyadenosine and C1 of the substrate can be 3.2 Å, which was estimated from the substrate radical-5′-methyl group model by electron spin echo envelop modulation (ESEEM) simulation (*36*).

Figures 2 and 3 show that enantiomeric 2-amino-1-propanols are bound to the active site of EAL in a similar manner except for the position of C3. The distances from C5′ of the adenosyl radical to C1-H_R, C1-H_S, and C2-H of the (*R*)-enantiomer are 3.8, 2.0, and 4.1 Å, respectively. The C4′−C5′−H_S (C1) angle is 108°. On the other hand, the distances from C5′ to C1-H_R, C1-H_S, and C2-H of the (*S*)-enantiomer are 3.8, 2.0, and 3.5 Å, respectively. The C4′−C5′−H_S (C1) angle is 104°. From these distances and directions, it is quite reasonable to predict that the adenosyl radical abstracts the *pro-S* hydrogen atom from C1 of both enantiomers. This prediction is just as expected from the experimental results of Diziol et al. (*25*) mentioned above.

It should be noted that such a binding mode of EAL makes it possible for the catalytic radical to abstract the *pro-S* hydrogen atom, i.e., the nearest hydrogen in common from both enantiomers. This is in clear contrast to the case for diol dehydratase, in which the radical center of the adenosyl radical comes closest to C1 of the enantiomeric 1,2-propanediols on the symmetrical plane, including O1, O2, and the substrate-coordinated metal ion (*23*). This metal ion was recently identified as calcium (*37*). As a result, the *pro-R* and *pro-S* hydrogens are abstracted by the adenosyl radical from the (*R*)- and (*S*)-enantiomers, respectively, in diol dehydratase.

Stereochemical Courses of the 1,2-Amino Group Migration. In panels A and B of Figure 3, the conformations of the enzyme-bound (*R*)- and (*S*)-2-amino-1-propanols viewed along

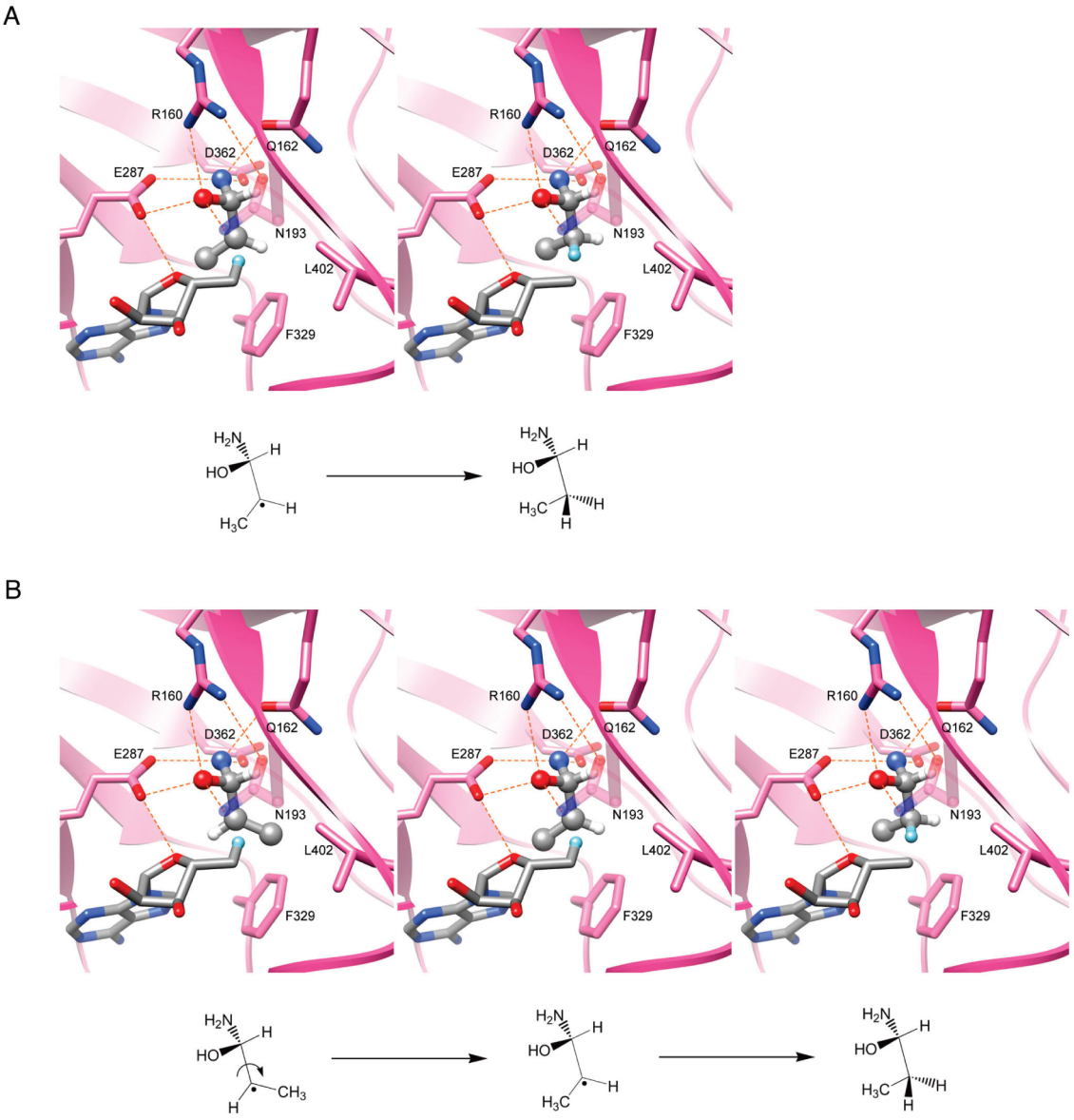

FIGURE 5: Postulated hydrogen back-abstraction steps. (A) Direct conversion from the (*R*)-enantiomer-derived 1-amino-1-propanol-2-yl radical to 1-amino-1-propanol. (B) Conversion from the (*S*)-enantiomer-derived 1-amino-1-propanol-2-yl radical to 1-amino-1-propanol through flipping at the C2 center. For the sake of clarity, cobalamin is not shown.

the C1−C2 bond are depicted in Newman projections. The O1−C1−C2−N2 torsion angles for the (*R*)- and (*S*)-enantiomers are 51.7° and 90.0°, respectively, both of which are characteristic of staggered conformations. The conformations of the 2-amino-1-propanol-1-yl radicals that would be formed by abstraction of the *pro-S* hydrogen from the (*R*)- and (*S*)-substrates are shown in panels A and B of Figure 4, respectively. It is reasonable to assume that the NH_2 group in the radical intermediates migrates from C2 to C1 by a suprafacial shift, i.e., from the same side (*re* face in this case) of the sp^2 carbon atom, because the energy along this pathway would be minimized by overlapping of the radical p orbital and the C2−N2 σ orbital. It can thus be predicted that the NH_2 group migrates from C2 to C1 with inversion of configuration at C1 for both enantiomeric substrates, although the absolute configuration of the 1-amino-1-propanol intermediate is not yet known. The stereochemical inversion at C1 in the substitution of a hydrogen atom by the migrating group has been postulated for the EAL reaction by Diziol et al. (*25*) and for the diol dehydratase reaction by Smith et al. (*38*) and us (*23*).

Modeling Study of Hydrogen Back-Abstraction. In the EAL reaction, the 1-amino-1-propanol-2-yl radical, the product radical, back-abstracts (recombines) a hydrogen atom from the methyl group of 5′-deoxyadenosine. To solve the stereochemical course of the hydrogen back-abstraction, the structures of the product radicals from the (*R*)- and (*S*)-enantiomeric substrates were modeled. Because the hydrogen bonds are much stronger than the hydrophobic or van der Waals interactions between the substrate C−C−C backbone and the enzyme, the substrate NH_2 group on C2 would migrate to C1 with the hydrogen bonding with the active site residues maintained. If viewed from the position of Gluα287, the C1−C2 bond of both (*R*)- and (*S*)-enantiomers would rotate counterclockwise upon 1,2-migration of the NH_2 group. On the basis of these assumptions, we could build the models of the 1-amino-1-propanol-2-yl radicals that are formed from the (*R*)- and (*S*)-enantiomers; that is, the 1-amino-1-propanol-2-yl radical intermediates were rotated around the O1−N1 line, so that C2 may come closest to C5′ of the modeled enzyme-bound 5′-deoxyadenosine. As shown in

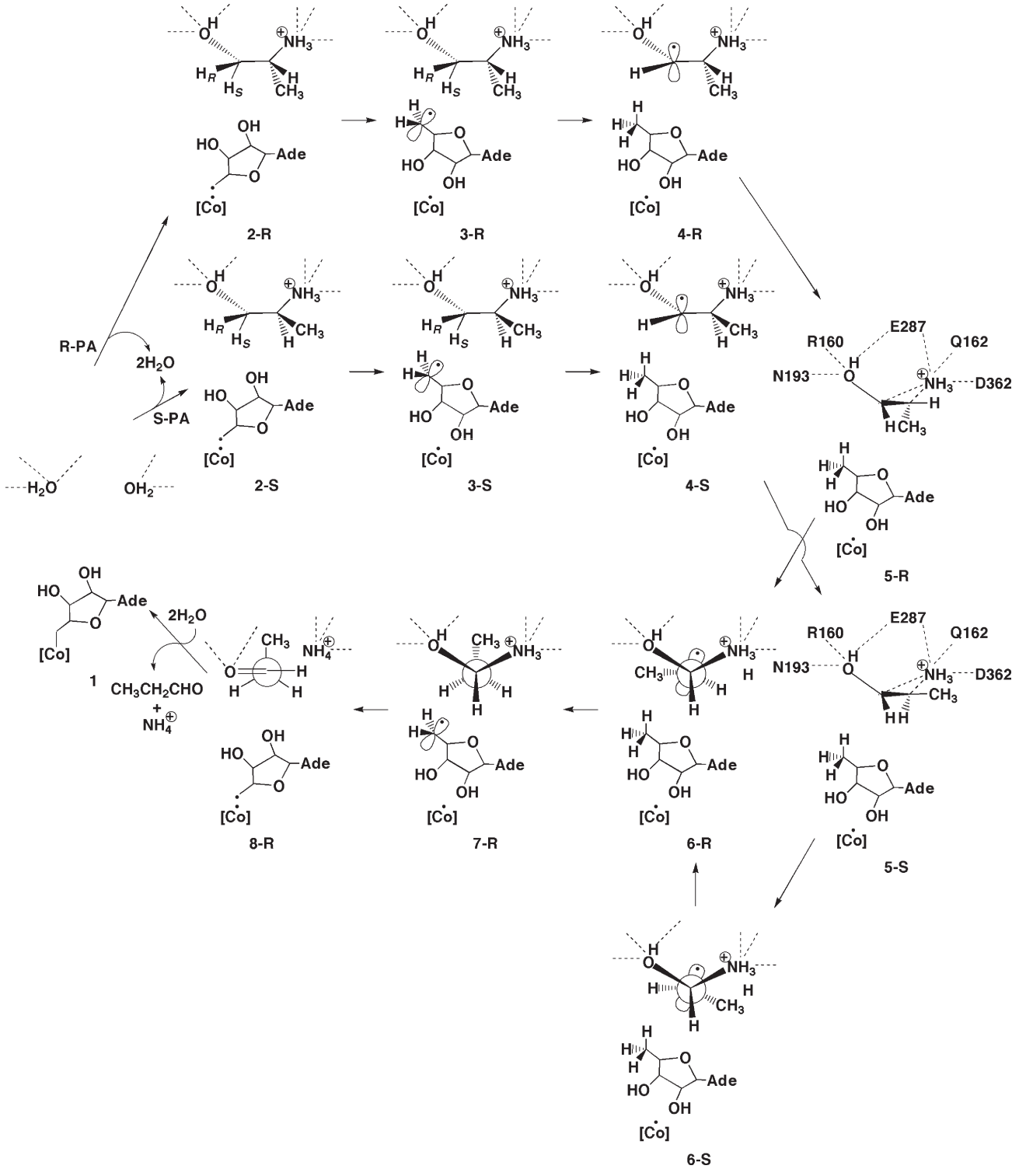

FIGURE 6: Stereochemical courses of the EAL reaction with (*R*)-2-amino-1-propanol (R-PA) and (*S*)-2-amino-1-propanol (S-PA) as substrates. [Co], cobalamin; Ade, 9-adeninyl group. Residue numbers are for the α subunit. H_R and H_S represent the *pro-R* and *pro-S* hydrogens, respectively.

the left panels of Figure 5, the binding conformations of the postulated product-radical intermediates from the (*R*)- and (*S*)-enantiomers would be similar except that the configurations at C2 would be inverted. Thus, they can be considered as rotameric isomers or rotamers. The distances from C5′ to C2 of the modeled 1-amino-1-propanol-2-yl radicals from the (*R*)- and (*S*)-enantiomeric substrate are 2.6 and 2.5 Å, respectively, and it was thus concluded that the hydrogen back-abstraction (recombination) from the CH_3 group of 5′-deoxyadenosine by the product radicals is structurally feasible.

Because the CH_3 group of 5′-deoxyadenosine is located on the opposite side from the migrating NH_2 group, it can be predicted that abstraction of hydrogen from the CH_3 group of 5′-deoxyadenosine by C2-centered product radicals would occur with inversion of configuration at C2 with both enantiomers. However, the experimental results of Diziol et al. (*25*) indicate that this is not always the case. Their labeling experiments demonstrate that (*R*)-2-amino-1-propanol is deaminated by EAL with inversion of configuration at C2 whereas the (*S*)-enantiomer with retention. Therefore, the prediction with the (*R*)-enantiomer

(Figure 5A) mentioned above is consistent with the experimental results, but that with the (*S*)-enantiomer is not. This strongly suggests that the radical intermediate from (*S*)-2-amino-1-propanol undergoes flipping or rotation around the C1−C2 axis to the rotamer from the (*R*)-enantiomer before hydrogen back-abstraction (Figure 5B). It is therefore likely that the active site of EAL has a preference for the rotameric intermediate from the (*R*)-enantiomer in equilibration. The molecular basis of this preference might be explained by the steric repulsion of C3 against the adjacent residues. That is, the C3 atom of the (*S*)-enantiomer-derived 1-amino-1-propanol-2-yl radical model has close contacts with Pheα329 (2.4 Å) and Leu402 (2.6 Å) (Figure 5B), whereas the contacts with Pheα329 (2.8 Å) and Leuα402 (4.5 Å) are not severe in the (*R*)-enantiomer-derived 1-amino-1-propanol-2-yl radical model (Figure 5A). Therefore, the severe contacts of the (*S*)-enantiomer-derived product radical at C3 with these residues would drive its flipping at C2 to the (*R*)-enantiomer-derived, less hindered conformation. The influence of Valα326 seems to be negligible because it is 3.5 and 4.7 Å from C3 of the (*R*)- and (*S*)-enantiomer-derived 1-amino-1-propanol-2-yl radical models, respectively. Poyner et al. (*8*) demonstrated via the ^{15}N isotope effects on EAL that the radical rearrangement steps, including ^{15}N-sensitive ones, make a significant contribution to V/K with the (*S*)-enantiomer. When chirally labeled (*R*)- and (*S*)-[2-^{2}H,^{3}H]ethanolamines are used as substrates, racemization takes place (*26*), which was explained by the torsion symmetry of the trigonal methylene radicals arising from this substrate.

In the case of diol dehydratase, ethylene glycols stereospecifically labeled with deuterium and tritium are converted to acetaldehyde with racemization (*39*), but (*R*)- and (*S*)-1,2-propanediols undergo dehydration in stereospecific manners (*1*−*3*). These results suggest that rapid internal rotation in the product radical occurs with ethylene glycol before hydrogen back-abstraction, but not with 1,2-propanediols. It is likely that, unlike EAL, the active site of diol dehydratase does not permit either symmetrization or equilibration of the 1,1-propanediol-2-yl radical intermediates.

Overall Mechanism and Stereochemical Courses of the EAL Reaction. On the basis of the X-ray structures and modeling studies, we propose here the overall mechanism and stereochemical courses of the EAL reaction with (*R*)- and (*S*)-2-amino-1-propanols as substrates (Figure 6). When each enantiomeric substrate is added, two water molecules in the active site (*22*) are displaced by its OH and NH_2 groups. The addition of substrate induces the additional labilization of the already activated Co−C bond of the coenzyme (*22*) and shifts the equilibrium toward its homolysis (*40*) to form a much more stable substrate radical from the highly reactive adenosyl radical. The C5′-centered radical is far from the substrate but comes close to the substrate by the ribosyl rotation around the glycosidic linkage. The radical abstracts the nearest hydrogen atom, i.e., *pro-S* hydrogen on C1 of both enantiomeric substrates, forming a substrate-derived radical and 5′-deoxyadenosine. The substrate radicals from both enantiomers would be subjected to migration of the NH_2 group from C2 to C1 through a similar cyclic transition state. During this step, the positions of the OH and NH_2 groups would be maintained and the C1−C2 bond would rotate counterclockwise, so that the new radical center C2 of the product radicals comes close to the CH_3 group of 5′-deoxyadenosine. Because the active site favors the rotameric radical intermediate from the (*R*)-enantiomer, the rotamer from the (*S*)-enantiomer undergoes flipping at C2 in equilibration before hydrogen back-abstraction. As a result, hydrogen back-abstraction produces exactly the same 1-amino-1-propanol from both (*R*)- and (*S*)-2-amino-1-propanol, although each follows a different stereochemical course depending upon the absolute configuration of C2. Finally, the 1-amino-1-propanol formed is subjected to elimination of ammonia to form the final product propionaldehyde and then leaves the active site by being displaced by water molecules. This would shift the equilibrium in favor of the recombination of the adenosyl radical and cob(II)alamin to regenerate the coenzyme. The protonation status of the NH_2 group during reaction has not yet been established.

SUPPORTING INFORMATION AVAILABLE

Summary of X-ray data collection and refinement statistics (Table S1) and overall architecture of EAL (Figure S1). This material is available free of charge via the Internet at http://pubs.acs.org.

REFERENCES

1. Zagalak, B., Frey, P. A., Karabatsos, G. L., and Abeles, R. H. (1966) The stereochemistry of the conversion of D and L 1,2-propanediols to propionaldehyde. *J. Biol. Chem. 24*, 3028–3035.
2. Rétey, J., Umani-Ronchi, A., Seibl, J., and Arigoni, D. (1966) On the mechanism of the propanediol dehydrase reaction. *Experientia 22*, 502–503.
3. Rétey, J., Umani-Ronchi, A., and Arigoni, D. (1966) Zur Stereochemie der Propandioldehydrase-Reaktion. *Experientia 22*, 72–73.
4. Yamane, T., Kato, T., Shimizu, S., and Fukui, S. (1966) Comparison of reactivity between D-propanediol and L-propanediol in intramolecular oxidation-reduction catalyzed by dioldehydrase requiring cobamide coenzyme. *Arch. Biochem. Biophys. 113*, 362–366.
5. Jensen, F. R., and Neese, R. A. (1975) Relative enantiomer binding and reaction rates with propanediol dehydrase. *Biochem. Biophys. Res. Commun. 62*, 816–821.
6. Bachovchin, W. W., Eagar, R. G., Jr., Moore, K. W., and Richards, J. H. (1977) Mechanism of action of adenosylcobalamin: Glycerol and other substrate analogs as substrates and inactivators for propanediol dehydratase—Kinetics, stereospecificity, and mechanism. *Biochemistry 16*, 1082–1092.
7. Graves, S. W., Fox, J. A., and Babior, B. M. (1980) Deamination of 2-aminopropanol by ethanolamine ammonia-lyase, an AdoCbl-requiring enzyme. Kinetics and isotope effects for the *R* and *S* enantiomers of the substrate. *Biochemistry 19*, 3630–3633.
8. Poyner, R. R., Anderson, M. A., Bandarian, V., Cleland, W. W., and Reed, G. H. (2006) Probing nitrogen-sensitive steps in the free-radical-mediated deamination of amino alcohols by ethanolamine ammonia-lyase. *J. Am. Chem. Soc. 128*, 7120–7121.
9. Bradbeer, C. (1965) The clostridial fermentations of choline and ethanolamine. II. Requirement for a cobamide coenzyme by an ethanolamine deaminase. *J. Biol. Chem. 240*, 4675–4681.
10. Lee, H. A., Jr., and Abeles, R. H. (1963) Purification and properties of dioldehydrase, an enzyme requiring a cobamide coenzyme. *J. Biol. Chem. 238*, 2367–2373.
11. Toraya, T., Shirakashi, T., Kosuga, T., and Fukui, S. (1976) Substrate specificity of coenzyme B_{12}-dependent diol dehydrase: Glycerol as both a good substrate and a potent inactivator. *Biochem. Biophys. Res. Commun. 69*, 475–480.
12. Abeles, R. H. (1979) Current status of the mechanism of action of B_{12}-coenzyme. In Vitamin B_{12} (Zagalak, B., and Friedrich, W., Eds.) pp 373−388, Walter de Gruyter, Berlin.
13. Toraya, T. (2003) Radical catalysis in coenzyme B_{12}-dependent isomerization (eliminating) reactions. *Chem. Rev. 103*, 2095–2127.
14. Babior, B. M. (1982) Ethanolamine ammonia-lyase. In B_{12} (Dolphin, D., Ed.) Vol. 2, pp 263−287, John Wiley & Sons, New York.
15. Bandarian, V., and Reed, G. H. (1999) Ethanolamine ammonia-lyase. In Chemistry and Biochemistry of B_{12} (Banerjee, R., Ed.) pp 811−833, John Wiley & Sons, New York.
16. Frey, P. A. (2010) Cobalamin coenzymes in enzymology. In Comprehensive Natural Products II Chemistry and Biology (Mander, L., and Lui, H.-W., Eds.) pp 501−546, Elsevier, Oxford, U.K.
17. Wagner, O. W., Lee, H. A., Jr., Frey, P. A., and Abeles, R. H. (1966) Studies on the mechanism of action of cobamide coenzymes. Chemical properties of the enzyme-coenzyme complex. *J. Biol. Chem. 249*, 1751–1762.

18. Schwartz, P. A., and Frey, P. A. (2007) Dioldehydrase: An essential role for potassium ion in the homolytic cleavage of the cobalt-carbon bond in adenosylcobalamin. *Biochemistry 46*, 7293–7301.
19. Magnusson, O. T., and Frey, P. A. (2002) Interactions of diol dehydrase and 3′,4′-anhydroadenosylcobalamin: Suicide inactivation by electron transfer. *Biochemistry 41*, 1695–1702.
20. Kaplan, B. H., and Stadtman, E. R. (1968) Ethanolamine deaminase, a cobamide coenzyme-dependent enzyme. II. Physical and chemical properties and interaction with cobamides and ethanolamine. *J. Biol. Chem. 243*, 1794–1803.
21. Shibata, N., Masuda, J., Morimoto, Y., Yasuoka, N., and Toraya, T. (2002) Substrate-induced conformational change of a coenzyme B_{12}-dependent enzyme: Crystal structure of the substrate-free form of diol dehydratase. *Biochemistry 41*, 12607–12617.
22. Shibata, N., Tamagaki, H., Hieda, N., Akita, K., Komori, H., Shomura, Y., Terawaki, S., Mori, K., Yasuoka, N., Higuchi, Y., and Toraya, T. (2010) Crystal structures of ethanolamine ammonia-lyase complexed with coenzyme B_{12} analogs and substrates. *J. Biol. Chem. 285*, 26484–26493.
23. Shibata, N., Nakanishi, Y., Fukuoka, M., Yamanishi, M., Yasuoka, N., and Toraya, T. (2003) Structural rationalization for the lack of stereospecificity in coenzyme B_{12}-dependent diol dehydratase. *J. Biol. Chem. 278*, 22717–22725.
24. Carty, T. J., Babior, B. M., and Abeles, R. H. (1974) The mechanism of action of ethanolamine ammonia-lyase, a B_{12}-dependent enzyme. Evidence for two intermediates in the catalytic process. *J. Biol. Chem. 249*, 1683–1688.
25. Diziol, P., Haas, H., Rétey, J., Graves, S. W., and Babior, B. M. (1980) The substrate-dependent steric course of the ethanolamine ammonia-lyase reaction. *Eur. J. Biochem. 106*, 211–224.
26. Rétey, J., Suckling, C. J., Arigoni, D., and Babior, B. M. (1974) The stereochemistry of the reaction catalyzed by ethanolamine ammonia-lyase, an adenosylcobalamin-dependent enzyme. An example of racemization accompanying substitution. *J. Biol. Chem. 249*, 6359–6360.
27. Shibata, N., Tamagaki, H., Ohtsuki, S., Hieda, N., Akita, K., Komori, H., Shomura, Y., Terawaki, S., Toraya, T., Yasuoka, N., and Higuchi, Y. (2010) Expression, crystallization and preliminary X-ray crystallographic study of ethanolamine ammonia-lyase from *Escherichia coli*. *Acta Crystallogr. F66*, 709–711.
28. Otwinowski, Z., and Minor, W. (1997) Processing of X-ray diffraction data collected in oscillation mode. *Methods Enzymol. 276*, 307–326.
29. Collaborative Computational Project, Number 4 (1994) The CCP4 suite: Programs for protein crystallography. *Acta Crystallogr. D50*, 760–763.
30. Emsley, P., and Cowtan, K. (2004) Coot: Model-building tools for molecular graphics. *Acta Crystallogr. D60*, 2126–2132.
31. Pettersen, E. F., Goddard, T. D., Huang, C. C., Couch, G. S., Greenblatt, D. M., Meng, E. C., and Ferrin, T. E. (2004) UCSF Chimera: A visualization system for exploratory research and analysis. *J. Comput. Chem. 25*, 1605–1612.
32. Chen, V. B., Arendall, W. B., III, Headd, J. J., Keedy, D. A., Immormino, R. M., Kapral, G. J., Murray, L. W., Richardson, J. S., and Richardson, D. C. (2010) MolProbity: All-atom structure validation for macromolecular crystallography. *Acta Crystallogr. D66*, 12–21.
33. Brunger, A. T., Adams, P. D., Clore, G. M., DeLano, W. L., Gros, P., Grosse-Kunstleve, R. W., Jiang, J. S., Kuszewski, J., Nilges, M., Pannu, N. S., Read, R. J., Rice, L. M., Simonson, T., and Warren, G. L. (1998) Crystallography & NMR system: A new software suite for macromolecular structure determination. *Acta Crystallogr. D54*, 905–921.
34. Markley, J. L., Bax, A., Arata, Y., Hilbers, C. W., Kaptein, R., Sykes, B. D., Wright, P. E., and Wüthrich, K. (1998) Recommendations for the presentation of NMR structures of proteins and nucleic acids. *Pure Appl. Chem. 70*, 117–142.
35. Masuda, J., Shibata, N., Morimoto, Y., Toraya, T., and Yasuoka, N. (2000) How a protein generates a catalytic radical from coenzyme B_{12}: X-ray structure of a diol-dehydratase−adeninylpentylcobalamin complex. *Structure 8*, 775–788.
36. Warncke, K., and Utada, A. S. (2001) Interaction of the substrate radical and the 5′-deoxyadenosine-5′-methyl group in vitamin B_{12} coenzyme-dependent ethanolamine deaminase. *J. Am. Chem. Soc. 123*, 8564–8572.
37. Toraya, T., Honda, S., and Mori, K. (2010) Coenzyme B_{12}-dependent diol dehydratase is a potassium ion-requiring calcium metalloenzyme: Evidence that the substrate-coordinated metal ion is calcium. *Biochemistry 49*, 7210–7217.
38. Smith, D. M., Golding, B. T., and Radom, L. (1999) Toward a consistent mechanism for diol dehydratase catalyzed reactions: An application of the partial-proton-transfer concept. *J. Am. Chem. Soc. 121*, 5700–5704.
39. Arigoni, D. (1979) A stereochemical approach to the diol dehydratase reaction. In Vitamin B_{12} (Zagalak, B., and Friedrich, W., Eds.) pp 389−410, Walter de Gruyter, Berlin.
40. Bandarian, V., and Reed, G. H. (2000) Isotope effects in the transient phases of the reaction catalyzed by ethanolamine ammonia-lyase: Determination of the number of exchangeable hydrogens in the enzyme-cofactor complex. *Biochemistry 39*, 12069–12075.